



PERGAMON

Progress in Particle and Nuclear Physics 42 (1999) 99-108

**Progress in
Particle and
Nuclear Physics**

Fluctuations in the Production of Intermediate Mass Fragments in Heavy Ion Collisions

W. BAUER,* T. GHARIB and S. PRATT

National Superconducting Cyclotron Laboratory and Department of Physics and Astronomy, Michigan State University, East Lansing, MI 48824-1321, USA

We study the the fluctuations in the number of intermediate mass fragments produced in heavy ion collisions. Of particular recent interest are the questions of scaling and reducibility of the probability distribution function of this observable. We show that the observed reducibility is a spurious effect, due to finite-number effects and the correlation between the measured transverse energy and the total charge recovered in the detector. Using only very simple assumptions, we are able to reproduce the observed binomial emission probabilities and their dependencies on the transverse energy. Finally, using the percolation model, we also show that useful information on the mechanism of intermediate mass fragment emission can be extracted from completely reconstructed events.

1 Introduction

During the last decade the main emphasis of relativistic and ultra-relativistic heavy ion physics has been the study of the phase diagram of nuclear matter and transitions between the phases. The main transitions believed to be observable in nuclear physics are the nuclear fragmentation transition between the nuclear liquid and a hadron gas, the transition between a hadron gas and a quark-gluon plasma, and the chiral restoration transition. Lattice QCD calculations indicate presently that the latter two transitions may occur at the same value of the control parameters. For all of these transitions, the investigation of fluctuation phenomena is essential.

Here we wish to focus our attention to the fragmentation phase transition. Since the elementary nucleon-nucleon interaction is repulsive at short and attractive at intermediate distances, we expect the nuclear phase-diagram to show a Van-der-Waals "liquid-gas" phase transition of first order, terminating in a second-order transition at the critical point. Recent observations report evidence for both, first and second order transitions.

In experiments studying Au-Au collisions conducted at the GSI, a measurement of the temperature as a function of excitation energy found possible evidence for a two-phase coexistence regime [1], not unlike the scenarios predicted by statistical multifragmentation models with excluded volume

*Email: bauer@nscl.msu.edu; url: <http://www.nscl.msu.edu/~bauer>

[2]. Other experiments conducted at the Bevalac focussed on the extraction of critical exponents from (almost) completely reconstructed Au-fragmentation events on C-targets, studying the dependence of the second moment of the charge distribution and size of the largest fragment as a function of the total charged particle multiplicity [3]. It was shown [4] that these data are consistent with the second-order phase transition predicted by the nuclear percolation model [5, 6].

If one wants to gain a fundamental understanding of the fragmentation process that goes beyond simple equilibrium model descriptions of the phenomena, then a proper description of the origin and time evolution of fluctuations is essential [2, 7, 8, 9]. In particular one wants to understand why particular molecular dynamics codes [10] produce fragments, and how these codes are connected to the fundamental processes of nuclear fragmentation.

2 Binomial Probability Distributions, Reducibility, Scaling

Moretto *et al.* [11] studied the mean and variance of the probability distribution as a function of total transverse energy, $E_t \equiv \sum_{\ell} E_{\ell} \sin^2 \theta_{\ell}$, where E_{ℓ} is the kinetic energy of particle ℓ . They found that the probability P_n of emitting n intermediate mass fragments (IMFs) follows a binomial distribution

$$P_n(m, p) = \frac{m!}{n!(m-n)!} p^n (1-p)^{m-n} \quad (1)$$

The parameters m and p are related to the average and variance of the distribution,

$$\langle n \rangle = \sum_{n=0}^{\infty} n P_n(m, p) = m \cdot p \quad (2)$$

$$\sigma^2 = \sum_{n=0}^{\infty} (n - \langle n \rangle)^2 P_n(m, p) = m p (1-p) \quad (3)$$

This suggest that p could be considered the elementary probability for the emission of one fragment, and the parameter m as the total number of tries, indicating that the problem of multi-fragment emission is reducible to that of multiple one-fragment emission. The claim for reducibility and its interpretation as the consequence of a simple barrier penetration phenomenon was further strengthened by the observation that $\ln(p^{-1})$ has a linear dependence on $1/\sqrt{E_t}$. Finally, the same scaling was found for different beam energies and different projectile-target combinations.

A prolonged discussion of these data and their interpretation in the literature [12] has pointed out some inconsistencies, but failed to put forward an alternative explanation to the one given by Moretto *et al.* Suggestions, for example, that the scaling and reducibility results from autocorrelations between the total transverse energy and that contained in the IMFs were shown to be not correct, because the same analysis also works, if the IMFs' transverse energy is excluded from the data.

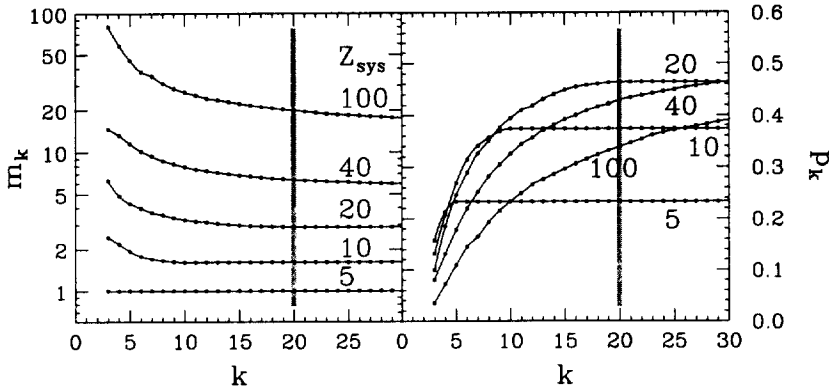


Figure 1: Dependence of the binomial parameters p and m on the upper mass number limit, k , of the summation over intermediate mass fragments, for different total charges of the fragmenting system, Z_{sys} .

3 Origin of the Observed Sub-Poissonian Statistics

We have found that the regularities and scalings found in the IMF probability distribution data can be explained as resulting from finite size effects, and by the effects of imperfect event reconstruction due to detector inefficiencies [13]. In order to show this as model-independent as possible, let us start with generating a random fragment distribution that is power-law distributed,

$$N(Z) \propto Z^{-\tau} \tag{4}$$

where Z is the fragment charge, and τ is the power-law exponent. We wish to generate events with exactly Z_{sys} charges. If an event has less than Z_{sys} charges, we add another fragment; if it has more than Z_{sys} charges, we discard the event. For an infinite system, this procedure results in the multiplicity distributions for individual fragments of a given Z to follow a Poisson distribution,

$$Q_n(\lambda) = \frac{\lambda^n \exp(-\lambda)}{n!} \quad \text{with: } \lambda = \langle n \rangle = \sigma^2 \tag{5}$$

And since the combined probability distribution of two Poisson-distributed variables is again a Poissonian, the multiplicity distribution of the total number of intermediate mass fragments (IMFs) is also Poissonian.

However, for any finite value of Z_{sys} , we cannot obtain an exact Poisson distribution. Thus the probability distributions in our simulation for finite Z_{sys} are closer to a binomial distribution with rather large values of m and small values of p . (When $m \rightarrow \infty$, $p \rightarrow 0$ such that $mp = \text{const.}$, we obtain a Poissonian as the limit of a binomial distribution.)

We now need to convolute these approximately binomial distributions for individual fragment charges to find the distribution of IMFs. To generate the IMF distributions, we sum over the probability

distributions of all fragments with charge $Z = 3$ to $Z = k$. ($k = 20$ corresponds to the usual IMF definition – gray bars in Fig. 1). The result of this procedure is a distribution that is still approximately binomial for all values of k . In Fig. 1, we show the values of p_k and m_k extracted as a function of the upper summation limit k . For this figure, a value of $\tau = 2.5$ was used, but other value of τ yield qualitatively similar results.

This figure clearly shows that for all values of Z_{sys} , p_k monotonically increases and m_k decreases with k . It also shows that p_k and m_k saturate for $k \geq Z_{\text{sys}}$. This is obvious, because there cannot be an IMF of size larger than Z_{sys} . For $k = 20$, we obtain the dependence of the extracted values of the binomial parameters as a function of system size, for any model that has a Poissonian IMF distribution in the limit of infinite system size.

In the studies of Moretto *et al.*, the binomial parameters are displayed as a function of transverse energy, E_t . In [13], we point out the correlation between Z_{sys} , the total charge recovered in the detector in a given event, and E_t , the total transverse energy measured in that event. We will not repeat this argument here, but simply state the result: The mean value of Z_{sys} rises linearly with E_t ,

$$\langle Z_{\text{sys}}(E_t) \rangle \approx 2 + 0.092 E_t/\text{MeV} \quad (6)$$

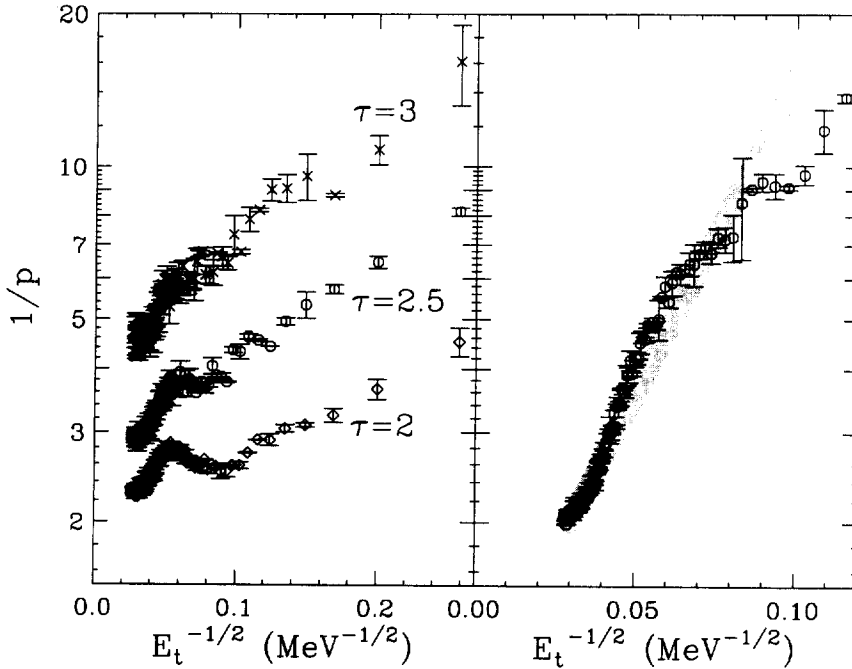


Figure 2: (*left*): Dependence of the binomial parameter p of the IMF distribution on the transverse energy for three different values of τ . (*right*): Dependence of the binomial parameter p of the IMF distribution on the transverse energy, assuming that the effective power τ of the fragment probability increases linearly with transverse energy. Plot symbols with error bars represent our calculations, the gray bar is a fit to the experimental data of Moretto and collaborators.

for values of E_t less than 0.7 GeV, and saturation for larger values. The width of the $Z_{\text{sys}}(E_t)$ -distribution is significant, typically on the order of 10 units of charge. While this result was communicated to us by M.B. Tsang specifically for the MSU Miniball detector employed in the experiments analyzed by Moretto et al., it is typical for most 4π detectors: projectile remnants move down the beam pipe, target remnants get stuck in the target frame, and both remain undetected. (This, by the way, is the argument that makes E_t a good filter for impact parameter.)

This connection between Z_{sys} and E_t already enables us to predict what the dependence of the binomial parameters on the transverse energy should be, assuming that we start with a model that has a power-law distributed fragment charge spectrum. The result is an approximately linear dependence of $\ln(p^{-1})$ on $1/\sqrt{E_t}$ [13]. This can be observed in the left panel of Fig. 2, where we display the result of our calculations for three fixed values of τ .

In the right panel of this figure, we assume that τ varies as a function of impact parameter, and with it as a function of E_t . This variation agrees with what is found experimentally [14]. We assume

$$\tau(E_t) = 3.5 - E_t/(0.5 \text{ GeV}) , \tag{7}$$

but the exact form of $\tau(E_t)$ is not very important. (We selected this particular dependence to obtain a physically reasonable value of $\tau \approx 2$ in central collisions.)

In Fig. 3 we show that the fragment multiplicity probability distributions that result from the

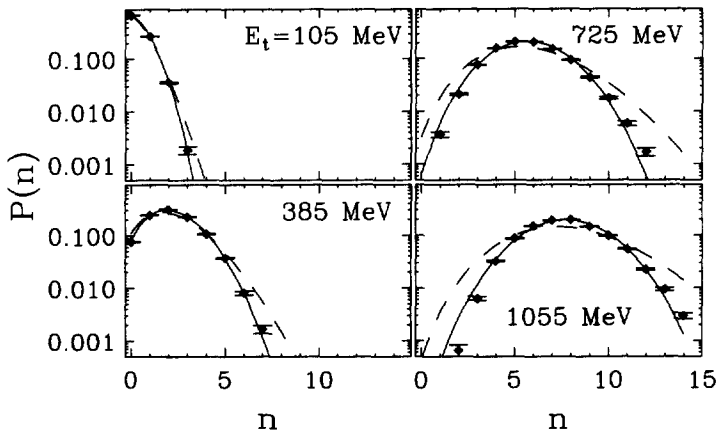


Figure 3: Probability distribution to obtain exactly n intermediate mass fragments in a given event for the reaction 55 AMeV Kr+Au, displayed for 4 representative values of the total transverse energy detected. The results of our calculations are displayed as the plot symbols with statistical error bars. The mean number of IMFs emitted at these 4 values of E_t are 0.35, 2.20, 5.72, and 7.75, respectively. Also shown are Poisson (dashed) and binomial (solid lines) fits to the results of our calculations.

procedures outlined above indeed are approximately binomial. The parameters of the calculation are the same as those entering the right panel of Fig. 2. The results of our calculations are shown by the plot symbols with statistical error bars. Also indicated are Poissonian (dashed lines) and binomial (solid lines) fits to our results. It is clear from this figure, that the IMF number probability distributions are - to good approximation - binomial for all values of the transverse energy. This binomial character, however, is not the result of some fundamental emission process. Instead it is almost exclusively the result of finite source size and incomplete detection efficiency effects. The observed scaling in the experimental data is thus not a signature of thermal scaling, as claimed by Moretto *et al.* [15].

4 Effects of Event Binning

Even though the main message up to now is that the E_t -dependence of the extracted binomial parameters of the fragment multiplicity distributions can be explained rather straightforwardly, we do not wish to convey the impression that there is no interesting information that one can extract from this type of analysis.

Here we consider the predictions of the bond-percolation model of nuclear fragmentation (nucleons are represented by sites on a 3-d lattice, connected to their nearest neighbors via bonds, which can be broken proportional to the amount of energy deposited) [5, 4], where we examine the difference between the mean and the variance of the IMF probability distribution. To do this, we define a quantity μ , the difference of the variance and the mean, normalized by the ratio, $N_{sites}/\langle n \rangle^2$.

$$\mu \equiv \frac{N_{sites}}{\langle n \rangle^2} (\sigma^2 - \langle n \rangle). \quad (8)$$

By dividing by $\langle n \rangle^2$, this normalization allows one to view the correlation even when fragment production is rare, and by multiplying by N_{sites} , μ becomes independent of the lattice size for large lattices. Positive and negative values of μ refer to super- and sub-Poissonian distributions, respectively.

In Fig. 4, we show [9] that the outcome of the fluctuation analysis is dependent on the way that the events in the sample are binned. A clear transition from sub-Poissonian to super-Poissonian is observed, when the breaking probability, p_b , is specified, and the events are binned according to this control parameter. This is shown by the circles in Fig. 4. (For reference, the 3-d bond percolation model exhibits a second-order phase transition at the critical value, $p_b^c = 1 - 0.2448 = 0.7552$.)

Instead of breaking each bond with probability p_b , one can break a fixed percentage of the bonds. This is equivalent to the micro-canonical limit (fixed total energy), whereas the procedure outline above is equivalent to the canonical limit (fixed temperature). Here, the multiplicity distributions (squares in Fig. 4) remain sub-Poissonian for the entire range of p_b . This binning procedure thus introduces an additional negative correlation, because the presence of an IMF of type a expended some of the broken bonds. This correlation is non-local as fragments far away from a are less likely to be produced.

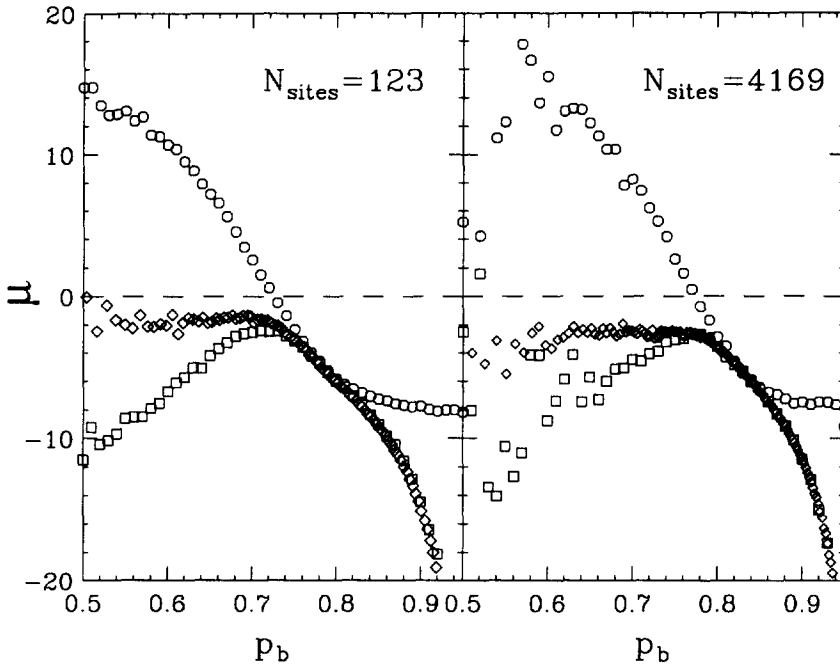


Figure 4: Scaled difference between the variance and mean, μ , as a function of the breaking probability, p_b , in the percolation model. Three different binning of the events were employed: collecting events with the same breaking probability of individual bonds (circles), collecting events with the same overall fraction of broken bonds (squares), and collecting events with the same value for the total multiplicity (diamonds, p_b was determined in this case as the average over all of the individual events entering a bin). (Left): small lattice with 123 sites. For this graph, a total of 10^5 events were generated. (Right): larger lattice with 4169 sites. 10^4 events were generated.

One might also bin events by the overall multiplicity of fragments of any size rather than by p_b . This has the advantage of offering a convenient means of comparing model calculations to experimental results. But it also introduces a negative correlation as the existence of an IMF of type a reduces the net number of other fragments by one, making the existence of a second IMF less likely. The results of such a binning are displayed by the diamonds in Fig. 4. The calculations for this binning were performed by choosing p_b randomly between 0.4 and 1.0, then binning the event according to multiplicity, and finally using the average p_b of events with a given multiplicity as the horizontal axis. In this way, each diamond in Fig. 4 corresponds to a specific multiplicity, but covers a range of p_b values. Again the variance is pushed towards the sub-Poissonian range. This illustrates the general principle that any binning criteria that are autocorrelated with the number of IMFs push the IMF multiplicity distribution in sub-Poissonian direction.

5 Predictions for Future Experiments

We conclude this manuscript with a prediction for future fluctuation analyses of completely characterized events, such as the ones available in the data collected by the EoS collaboration at the Bevalac.

Using a TPC, the EoS collaboration [3] has managed to provide a sample of more than 10^4 events for the fragmentation of a 1 AGeV gold beam by a carbon target, in which all (or almost all) charges contained in the gold nucleus were recovered. Previously, we have shown that the outcome of this experiment can be reproduced very well by a hybrid INC-percolation model, in which the first fast step of this reaction is modeled by an intra-nuclear cascade (INC) calculation which predicts the amount of energy deposited and the size of the residue, and in which a percolation stage uses these as input to predict the fragment formation [4].

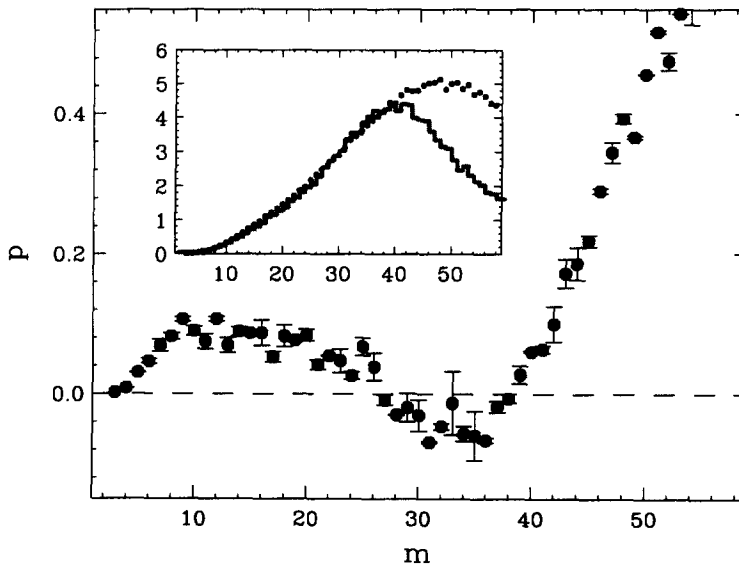


Figure 5: Prediction for the values of the binomial parameter p as a function of the total multiplicity, m , of charged particles, for the reaction 1 AGeV Au+C, for completely reconstructed events. The inset show the mean number of IMF's (circles) and the variance of the number of IMF's (histogram) in individual events, as a function of total multiplicity of charged particles.

Since the events in the 1 AGeV Au + C reaction are completely characterized, they do not suffer from the problems we outlined above for the analysis of Moretto and collaborators. Thus a fluctuation analysis can provide additional valuable insight into the nature of the fragmentation process. In Fig. 5, we predict the outcome of such an analysis for the EoS TPC data, using our model. The horizontal

axis is the total charged particle multiplicity, and the vertical axis is the parameter p ,

$$p = 1 - \frac{\sigma^2}{\langle n \rangle} \begin{cases} = 0 & \Rightarrow \text{Poisson} \\ < 0 & \Rightarrow \text{Binomial} \\ > 0 & \Rightarrow \text{Negative Binomial} \end{cases} \quad (9)$$

The choice of p obviously is motivated by inversion of Eqs. 2 and 3, but can be universally extracted for sub- and super-Poissonian distributions.

The inset of Fig. 5 shows the values of the mean number of IMFs (black dots) and the variance in this variable (gray histogram) as a function of the total charged particle multiplicity.

The main prediction of this figure is that the IMF probability distributions will turn super-Poissonian for a small range of total charged particle multiplicities, slightly above the critical multiplicity. This prediction can be tested readily. A comparison of the experimental data with the predictions in Fig. 5 should enable us further determine if the percolation picture of nuclear fragmentation is the correct one.

Acknowledgments

This work was supported by the National Science Foundation, grant PHY-9605207. T. Gharib acknowledges support from the National Superconducting Cyclotron Laboratory during his research sabbatical visit to the USA.

References

- [1] J. Pochodzalla *et al.*, *Phys. Rev. Lett.* **75** (1995) 1040; J. Pochodzalla, *Prog. Part. Nucl. Phys.* **39** (1997) 443.
- [2] J. Randrup and S. Koonin, *Nucl. Phys. A* **356** (1981) 321; D.H.E. Gross, *Rep. Prog. Phys.* **53** (1990) 605; J.P. Bondorf, A.S. Botvina, A.S. Iljinov, I.N. Mishustin and K. Sneppen, *Phys. Rep.* **257** (1995) 133.
- [3] M.L. Gilkes *et al.*, *Phys. Rev. Lett.* **73** (1994) 1590; J.B. Elliott *et al.*, *Phys. Rev. C* **49** (1994) 3185; H.G. Ritter *et al.*, *Nucl. Phys. A* **583** (1995) 491c.
- [4] W. Bauer and W.A. Friedman, *Phys. Rev. Lett.* **75** (1995) 767; W. Bauer and A. Botvina, *Phys. Rev. C* **52** (1995) R1760; *Phys. Rev. C* **55** (1997) 546.
- [5] W. Bauer *et al.*, *Phys. Lett.* **B150** (1985) 53; W. Bauer *et al.*, *Nucl. Phys.* **A452** (1996) 699; W. Bauer, *Phys. Rev. C* **38** (1988) 1297.

- [6] X. Campi, J. Phys. A **19** (1986) L917.
- [7] W. Bauer, G.F. Bertsch, and S. Das Gupta, Phys. Rev. Lett. **58** (1987) 863.
- [8] Ph. Chomaz, Ann. Phys. France **21** (1996) 669; G.F. Burgio, Ph. Chomaz and J. Randrup, Phys. Rev. Lett. **69** (1992) 885.
- [9] T. Gharib, W. Bauer, and S. Pratt, Phys. Lett. B, in print; Michigan State University preprint, Los Alamos preprint archive nucl-th/9808065.
- [10] J. Aichelin and H. Stöcker, Phys. Lett. **B176** (1986) 14; D.H. Boal and J.N. Glosli, Phys. Rev. C **38** (1988) 2621; H. Feldmeier, Nucl. Phys. **A515** (1990) 147; J. Aichelin, Phys. Rep. **202** (1991) 233; A. Ono et al., Prog. of Theoret. Phys. **87** (1992) 1185; A. Ono et al., Phys. Rev. Lett. **68** (1992) 2898; V. Latora et al., Phys. Rev. Lett. **73** (1994) 1765; S. Pratt et al., Phys. Lett. **B349** (1995) 261; H. Feldmeier and J. Schnack, Prog. Part. Nucl. Phys. **39** (1997) 393; A. Ohnishi and J. Randrup, Phys. Lett. B **394** (1997) 260; D. Kiderlen and P. Danielewicz, Nucl. Phys. A **620** (1997) 46.
- [11] L.G. Moretto et al., Phys. Rev. Lett. **71** (1993) 3935; L.G. Moretto et al., Phys. Rev. Lett. **74** (1995) 1530; L. Phair et al., Phys. Rev. Lett. **77** (1996) 822; L.G. Moretto et al., Phys. Rep. **287** (1997) 249; L. Beaulieu et al., in Proceedings of the 14th Winter Workshop on Nuclear Dynamics, ed.: W. Bauer and H.G. Ritter (Plenum, New York, 1998), to be published.
- [12] A. Del Zoppo et al., Phys. Rev. Lett. **75** (1995) 2288; J. Toke, D.K. Agnihotri, B. Djerroud, W. Skulski and W.U. Schroeder, Phys. Rev. C **56** (1997) R1686; M.B. Tsang and P. Danielewicz, Phys. Rev. Lett. **80** (1998) 1178; L.G. Moretto, L. Bealieu, L. Phair, and G.J. Wozniak, Los Alamos preprint archive nucl-ex/9709001 (1997).
- [13] W. Bauer and S. Pratt, submitted for publication; MSU-NSCL preprint, Los Alamos preprint archive nucl-th/9808068 (1998).
- [14] T. Li et al. Phys. Rev. Lett. **70** (1993) 1924; T. Li et al. Phys. Rev. C **49** (1994) 1630; C. Williams et al., Phys. Rev. C **55** (1997) R2132.
- [15] We received an unpublished manuscript by O. Tirel, G. Auger, R. Nebauer, and J. Aichelin which comes to conclusions similar to ours by using the QMD model and the acceptance of the INDRA detector.